Structure, shape and single particle states of the Cd isotopes using relativistic mean field theory

البُنية والشكل ومستويات الطاقة لنظائر عنصر الكادميوم باستخدام نظرية المجال المتوسط النسبية

A thesis submitted in partial fulfillment

of the requirements for the Masters degree in Physics

Sondos Sa'd Qatu

Supervised by :

Dr. Hazem Abusara

BIRZEIT UNIVERSITY

Birzeit, Palestine

2019

Structure, shape and single particle states of the Cd isotopes using relativistic mean field theory

A thesis submitted in partial fulfillment

of the requirements for the Master's degree in Physics

By:

Sondos Sa'd Qatu

Thesis committee:

Dr. Hazem Abusara (Principle advisor)

Dr. Abdallah Sayyed-Ahmad (Member)

Dr. Wafaa Khater (Member)

Dedication

To my great parents who always strive to give the best in life for their love and eternal support and to my sisters and brothers for their continuous encouragement. To my life-partner for his great patience and help, without his support nothing could be achieved. To my new family, my husband family whose help has been motivating to do my best. To my wonderful friends who have been my sisters from another mother.

Acknowledgement

Firstly, I would like to express my sincere gratitude to my Thesis supervisor Dr. Hazem Abusara for his continuous support and assistance through my thesis research. I would also like to thank members of my committee, Dr. Wafaa khater and Dr. Abdallah Sayyed-Ahmad, for reviewing my thesis. Moreover, I would like to thank the physics department staff who have been amazing teachers and colleagues.

Abstract

Nuclear shape, single particle states and ground states properties such as binding energy, two neutron separation energy (S_{n2}), and proton and neutron radii in the Cd isotopic chain are studied within the framework of relativistic mean field theory using nonlinear meson nucleon coupling model. A systematic investigation of the ground state shape is also performed for Cd isotopes (Z=48, $47 \leq N \leq 116$). The shape of the ground state for Cd isotopes varies between three categories: spherical, axial (prolate, oblate) and triaxial. Our results suggest that the neutron deficient side of the chain exhibts an oblate-prolate transition, after that the shape fluctuations are between axial (oblate or prolate) and triaxial.

Single particle states are shown for nuclei, which have a jump in value of quadrupole deformation β_{20} and neighboring nuclei. Single particle states are in a good agreement with Nilsson Diagram for axial nuclei.

The physical properties: Binding energy, two neutron energy, neutron, proton, and charge radii are studied as a function of mass number. In general, a smooth change in these properties is found, except near A = 98, 130, 136, one can see a sharp change, which reflect the sudden change in the ground state deformation in the neighboring nuclei. Our calculations shows a reasonable agreement with experimental data.

الملخص

ندرُس في هذا البحث شكل الانوية ومستويات الطاقة والخصائص الفيزيائية كطاقة الربط، وطاقة فصل النيوترونات، ونصف قطر كل من البروتون والنيوترون في مستوى الطاقة الأرضي لنظائرعنصر الكادميوم باستخدام نظرية المجال المتوسط النسبية بالاعتماد على التفاعلات غير الخطية للنيوكليونات.

بناء على الحسابات التي قمنا بها لنظائر الكادميوم (العدد الذري:48 وعدد النيوكليونات من 47 الى 116) تبين أن هناك أشكالا هندسية مختلفة لأنوية نظائر الكادميوم في المستوى الأرضي، فمنها ما هو كرويَ الشكل تام، ومنها ما هو متماثل حول محوره " بشكل مفلطح أو متضخم " ومنها ما ينعدم تماثله المحوري بنسبة تشوه كبير عن الشكل الكروي

أيضا قمنا برسم مستويات الطاقة لبعض الانوية التي يوجد عندها قفزات في قيم معامل التشوه والانوية التي حولها، وتبين أن هناك توافقا بينها وبين مستويات الطاقة في مخطط نيلسون للأنوية ذات التماثل المحوري.

كذلك قمنا بدراسة الخصائص الفيزيائية كاقتران مع العدد الكتلي. لوحظ بشكل عام تغير متناسق فيها ماعدا عند بعض الانوية، حيث يوجد تغير حاد وذلك يعود الى التغير المفاجئ في شكل الانوية المجاورة لها. تظهر جميع حساباتنا توافق الى حد كبير مع النتائج العملية والنظريات الأخرى.

Table of Contents

List of Figure

CHAPTER ONE
Introduction

The World Nobel Prize was awarded for A. Bohr, B. Mottelson and L. Rainwater in 1975 because they discovered that the nucleus could have a non-spherical shape [1]. They provided invaluable tool to study this innovative concept (Nuclear Deformations) in their monograph Nuclear Structure Vol. II [2]. This phenomenon has been a focus of interest for many decades. One of the nuclei that has received a great interest in the scientific community to study its nuclear structure is Cd isotopes (Z=48). This is because they exhibit collective excitations and are located adjacent to the closed shell at (Z = 50) for the doubly magic Sn isotopes [3, 4].

Different techniques and nuclear models are used to study experimentally and theoretically the nuclear structure such as complete spectroscopy and coulomb excitation, interacting bosons model (IBM), relativistic and non-relativistic models using Hartree-Fock-Bogolibov (HFB) and self-consistent Hartree-Fock (HF) models[5,7,12,14].

The Coulomb excitation is a process of inelastic scattering in which a charged particle transmits energy to the nucleus through electromagnetic field [5] and it is directly related to the nuclear shape through measuring electromagnetic moments [6]. If the electromagnetic moments has a positive value, then the shape is a prolate, and when it has a negative value, then the shape is an oblate.

The other model is interacting boson model (IBM) [7]. It has been extended to cover most nuclear structure; it can be used to predict vibrational and rotational modes of non spherical nuclei [8]. In this model, nucleons pair up and behave like a single particle with boson properties. These boson are called s-boson or d-boson crossponding to the nucleon pairs are presented with angular momenta L= zero or 2, respectively[9].

In addition, mean field approximation are extensively applied in nuclear structure and it has been successfully used to study the ground-state properties of nuclei all over the nuclear chart. Mean field approximation depend on effective interaction, a zero range skyrme

force, finite range Gongy force[10,11] and also it depends on non-relativistic and relativistic realization self-consistent Hartree-Fock (HF) and Hartree-Fock-Bogolibov (HFB)models.

In the Hartree-Fock approach, the starting point is a Hamiltonian containing kinetic and potential terms. The wave function of the system can be written as a Slater determinant of one particle spin orbitals. The components of this Slater determinant (individual wave functions of the nucleons) are then determined. To this end, it is assumed that the total wave function (the Slater determinant) is such that the energy is minimum [12-14].

In relativistic Hartree-Fock-Bogolibov (RHFB), nucleons interact by exchange of virtual particles such as mesons. The problem is solved by firstly building the Lagrangian containing these interaction terms, then preparation a set of equations of motion for which the nucleons obey the Dirac equation, while the mesons obey the Klein-Gordon equation [14,16]. Finally, these equations are solved by expanding the different components of the quasi-particle spinors in the

complete set of Eigen solutions of the Dirac equations with Woods-Saxon potentials [15].

All these previous techniques and models were successfully applied to the study of shape evolution. Hossain et al. studied the nuclear structure of the ground state energy bands up to 8^+ in even-even Cd isotopes (Z=48 and N=56-74) using interacting boson model-1(IBM-1) and acceptable results were obtained as compared with recent experimental data [17]. In addition, Garrett wrote a review paper on the evolving structure of Cd isotopes. Early in the 1950s, even-even Cd isotopes were considered as a main example of vibrational behavior. Later in 1970's, shape coexistence and intruder states were noticed and recently many models were used to study this new behavior. However, by combining results from these studies, he suggested that the structure of Cd isotopes have deformed γ-soft rotors rather than spherical vibration [18].

Michael Hammen studied nuclear ground state properties of the isotopic chain of $^{100-130}$Cd. His work was based on nuclear shell model,

which is more accurate at the region nearby closed shell. Cd isotopes has 48 proton, which is two proton less than the shell closure that occurs at Z= 50 for Sn isotopes, and their isotopes from N = 52 up to N = 82 which cover complete region between the neutron shell closures N = 50 and N = 82, so nuclear shell model is acceptable here. He used experimental technique called collinear laser spectroscopy. Many properties like the magnetic dipole moments, the electric quadrupole moments, spins and changes in mean square charge radii are recorded from data and analysis. In addition other features are revealed from data obtained such as an extremely linear behavior of the quadrupole moments of the I = 11/2− isomeric states and a parabolic development in differences in mean square nuclear charge radii between ground and isomeric state. The development of charge radii between the shell closures is smooth, exposes a regular odd-even staggering and can be described and interpreted in the model of Zamick and Thalmi [19].

In 2014, Bespalova et al. calculated neutron energies E_{nlj} of Cd isotopes from N=50 to 82 and N=126 using dispersive optical potential taking into account the coupling of single particle motion with more

complicated configuration of the nucleus and the extracted features are in good agreement with experimental results. In addition, they calculated from these energies the occupation probabilities for neutron subshell using formula in the Bardeen–Cooper–Schrieffer (BCS) theory. As well, the results from calculations of ^{174}Cd isotope agree with the premise that this nucleus exhibits magic properties and is stable against decay with the emission of neutron [20].

In 2015, Blazhev et al. performed large-scale shell model (LSSM) calculations for the light even-even $^{98-108}$Cd isotopes in the proton ($2p_{1/2}$, $1g_{9/2}$) and the neutron ($2d_{5/2}$, $1g_{7/2}$, $2d_{3/2}$, $3s_{1/2}$, $1h_{11/2}$) model space. By comparing with experimental data, the lowest 2+ and 4+ states energies are the same, while the higher spin states show deviations in energy. In addition, the increasing collectivity in the light Cd isotopes when moving away from the N = 50 closed shell, appeared from calculations of R (4/2) ratio [21].

In 2018, K. C. Naik, et al. study the ground state properties of even-even Cd isotopes (N=56-86) using relativistic mean field theory using

two developed parameter sets FSU Garent and IOPB-I. Various physical quantities such as binding energy (BE), two-neutron separation energy (S_{2n}), root mean square (rms) radii, shell quenching at N = 82 for different Cd isotopes are calculated and compared with available experimental data [22].

Also, a systematic study of the ground-state properties of the entire chains of even–even neutron magic nuclei represented by isotones of traditional neutron magic numbers N = 8, 20, 40, 50, 82 and 126 has been carried out using **relativistic mean-field (RMF)** plus Bardeen-Cooper-Schrieffer (BCS) approach. The investigation includes deformation, binding energy, two-proton separation energy, single particle energy, rms radii along with proton and neutron density profiles, etc. Several of these results are compared with the results calculated using nonrelativistic approach (Skyrme–Hartree–Fock method) along with available experimental data and indeed, they are found with excellent agreement [23].

Moreover, K. Nomura and J. Jolie based on constrained self-consistent mean-field calculations with a choice of the Skyrme force and pairing property, onto the Hamiltonian of the interacting boson model. Deformation energy surfaces were calculated for the even-even $^{108-116}$Cd isotopes. This energy surfaces yielded both a prolate and a minor oblate minimum. The low-lying excitation spectra and electric quadrupole and monopole transition rates for the considered Cd nuclei are computed by the resultant Hamiltonian, and are compared in detail with the experimental data [24].

In the present analysis, we will perform a systematic calculation to investigate the shape evolution for Cd isotopes using the relativistic mean field theory using NL3* force and we will discuss the binding, separation energies for neutrons. Then we will discuss the results and compare it with other models.

This thesis is organized as follows: CHAPTER 2 contains the formalism of the model RMFT. CHAPTER 3 contains shape evoluation, single particle states and physical properties for the ground state of Cd isotopes. CHAPTER 4 presents summary and main result.

CHAPTER TWO
Formalism

2.1 Covariant density functional theory

Density functional is computational method providing a successful microscopic description for a large majority of nuclei. It is useful for determining the both properties of nuclear ground state such as radii, binding energy, deformation parameters and excited states such as rotational bands and collective vibrations [25-27].

Three types of models introduced to describe atomic nuclei in relativistic density functional density: the nonlinear meson nucleon-coupling model, the density-dependent meson nucleon-coupling model and a density-dependent point coupling model. The main difference between them is the treatment of the range of the interaction, the mesons, and density dependence. The interaction in the first two classes has a finite range, while the third class uses zero-range interaction.

In this work, we will use the first model which is the nonlinear meson nucleon-coupling model.

2.2 Lagrangian density for the mesons-exchange models

In the meson-exchange models, the nucleus is considered as a system of point like nucleon, Dirac spinors, interacting via the exchange of mesons with finite masses leading to the interactions of finite range.

We start from Lagrangian density:

$$\mathcal{L} = \mathcal{L}_{nucleon} + \mathcal{L}_{mesons} + \mathcal{L}_{int} \tag{2.1}$$

Lagrangian density of the free nucleon is described by:

$$\mathcal{L}_{nucleon} = \bar{\psi}\gamma(i\partial - m)\psi \tag{2.2}$$

Where m is the mass of nucleons, and ψ is the Dirac spinor.

Lagrangian density of mesons and electromagnetic field is given by:

$$\mathcal{L}_m = \frac{1}{2}\partial_\mu\sigma\partial_\mu\sigma - \frac{1}{2}m_\sigma^2\sigma^2 - \frac{1}{4}\Omega_{\mu\nu}\Omega^{\mu\nu} + \frac{1}{2}m_\omega^2\omega^2 - \frac{1}{4}\vec{R}_{\mu\nu}\vec{R}^{\mu\nu} + \frac{1}{2}m_\rho^2\vec{\rho}^2 - \frac{1}{4}F_{\mu\nu}F^{\mu\nu} \tag{2.3}$$

where

$$\Omega_{\mu\nu} = \partial_\mu\omega_\nu - \partial_\nu\omega_\mu \tag{2.4}$$

$$\vec{R}_{\mu\nu} = \partial_\mu\vec{\rho}_\nu - \partial_\nu\vec{\rho}_\mu \tag{2.5}$$

$$F_{\mu\nu} = \partial_\mu A_\nu - \partial_\nu A_\mu \tag{2.6}$$

and the lagrangian density of interaction between the nucleons and the mesons is given by:

$$\mathcal{L}_{int} = -\psi(g_\sigma\sigma + g_\omega\gamma^\mu\omega^\mu + g_\rho\vec{\tau}\gamma^\mu\rho_\mu + e\frac{1-\tau_3}{2}\gamma^\mu A_\mu)\psi \tag{2.7}$$

The nucleons interact by the exchange of several mesons. These mesons are defined by three quantum numbers; spin (J), parity (P) and isospin (T). Mesons that participate in this interaction are:

1. The isoscalar scalar σ -meson, has quantum numbers (J = 0, T = 0 and P =1), and the corresponding field is a scalar produce attraction.

2. The isoscalar vectorω-meson, has quantum numbers (J=1, T=0, P=-1), and the corresponding field is a vector produce the repulsion.

3. The isovector vector ρ- meson, has quantum numbers (J=1, T=1, P=-1), and it couple to the iso vector current.

Starting on a more fundamental level, one therefore introduces a relativistic Lagrangian describing point-like nucleons interacting through the exchange of different types of mesons.

$$\mathcal{L} = \bar{\psi}\left(\gamma\left(i\partial_\mu - g_\omega\omega - g_\rho\vec{\rho}\vec{\tau} - eA\right) - m - g_\sigma\right)\psi + \frac{1}{2}\partial\sigma\partial\sigma - \frac{1}{2}m_\sigma^2\sigma^2 - \frac{1}{4}\Omega_{\mu\nu}\Omega^{\mu\nu} + \frac{1}{2}m_\omega^2\omega^2 - \frac{1}{4}\vec{R}_{\mu\nu}\vec{R}^{\mu\nu} + \frac{1}{2}m_\rho^2\vec{\rho}^2 - \frac{1}{4}F_{\mu\nu}F^{\mu\nu} \quad (2.8)$$

It contains as parameters the meson masses m_σ,m_ω, and $m_\rho$and the coupling constantsg_σ, $g_\omega$and g_ρ, and e is the charge of the protons and it vanishes for neutrons.

To treat the density dependence in this model, Boguta and Bodmer[28] introduced a density dependence via a non-linear meson coupling replacing the term $\frac{1}{2}m_\sigma^2\sigma^2$ in (eq. 2.8) by:

$$U(\sigma) = \frac{1}{2}m_\sigma^2\sigma^2 + \frac{1}{3}g_2\sigma^3 + \frac{1}{4}g_3\sigma^4 \qquad (2.9)$$

The nonlinear meson nucleon coupling is represented by the parameter set NL3*[29, 30].

parameter	NL3*
M	939
m_σ	502.5742

g_σ	10.0944
m_ω	782.600
g_ω	12.8065
m_ρ	763.000
g_ρ	4.5748

Table 2.1 NL3* parameterizations of the RMF Lagrangian

2.3 The Hamiltonian and the equation of motion

From the lagrangian density in eq. (2.8) the Hamiltonian operator is:

$$H = \int \partial^3 r(\sum_m P_m - \partial_t \varphi_m - \mathcal{L}(m) \tag{2.10}$$

Where P_m is momentum conjugate operator

$$P_m = \frac{\partial \mathcal{L}}{\partial(\frac{\partial \varphi_m}{\partial t})} \tag{2.11}$$

And φ_m=$(\psi, \sigma, \omega_\mu, A_\mu, \vec{\rho}_\mu)$

So the total Hamiltonian is:

$$H = H_\psi + H_\sigma + H_\omega + H_\rho + H_A + H_{int} \tag{2.12}$$

Where:

$$H_{\psi} = \bar{\psi}(\alpha.p + Bm)\psi \tag{2.13}$$

$$H_{\sigma} = -\frac{1}{2}\sigma\Delta\sigma + U_{\sigma}(\sigma) \tag{2.14}$$

$$H_{\omega} = \frac{1}{2}\omega_{\mu}\omega^{\mu} - U_{\omega}(\omega) \tag{2.15}$$

$$H_{A} = \frac{1}{2}A_{\mu}A^{\mu} \tag{2.16}$$

$$H_{\rho} = \frac{1}{2}\vec{\rho}_{\mu}\Delta\vec{\rho}^{\mu} - U_{\rho}(\rho) \tag{2.17}$$

$$H_{int} = \bar{\psi}(g_{\sigma}\sigma + g_{\omega}\omega_{\mu}\gamma^{\mu} + g_{\rho}\vec{\rho}_{\mu}\gamma^{\mu}\vec{\tau} + e\frac{1-\tau_{3}}{2}A_{\mu}\gamma^{\mu})\psi \tag{2.18}$$

In the Haretree approximation, the stationary Dirac equation for the nucleons is:

$$\hat{h}_{D}\psi_{i} = \epsilon_{i}\psi_{i} \tag{2.19}$$

where $\hat{h}_D$is the Hamiltonian of the nucleons with mass m

$$\hat{h}_D = \alpha\left(-i\nabla - V(r)\right) + V_\circ(r) + B(m + S(r)) \tag{2.20}$$

the Hamiltonian contains the attractive scalar field S(r)

$$S(r) = g_\sigma \sigma(r) \tag{2.21}$$

and the repulsive time like component of the vector V_0(r)

$$V_\circ(r) = g_\omega \omega_\circ(r) + g_\rho \tau_3 \rho_\circ(r) + e\frac{1-\tau_3}{2} A_\circ(r) \tag{2.22}$$

and the magnetic potential V(r)

$$V(r) = g_\omega \omega(r) + g_\rho \tau_3 \rho(r) + e\frac{1-\tau_3}{2} A(r) \tag{2.23}$$

Note that in these equations, the four-vector components of the vector field $(\omega^\mu, \rho^\mu, A^\mu)$ are separated into the time-like $(\omega_\circ, \rho_\circ, A_\circ)$ and the space-like components $[\omega^x, \omega^y, \omega^z)$; $\rho = (\rho^x, \rho^y, \rho^z)$; A = ($A^x$, A^y, A^z)].

The corresponding mesons Fields and the electromagnetic field are determined by the Klein-Gordon equations:

$$(-\nabla^2 + m_\sigma^2)\sigma(r) = -g_\sigma \rho_s(r) - g_2\sigma^2(r) - g_3\sigma^3(r) \quad (2.24)$$

$$(-\nabla^2 + m_\omega^2)\omega_\circ(r) = g_\omega \rho_v \quad (2.25)$$

$$(-\nabla^2 + m_\omega^2)\omega_\mu(r) = g_\omega j_\mu \quad (2.26)$$

$$\left(-\nabla^2 + m_\rho^2\right)\rho_\circ(r) = g_\omega \rho_3 \quad (2.27)$$

$$\left(-\nabla^2 + m_\rho^2\right)\vec{\rho}_\mu(r) = g_\rho \vec{j}_\mu \quad (2.28)$$

$$-\nabla^2 A_\circ(r) = e\rho_p(r) \quad (2.29)$$

$$-\nabla^2 A_\mu(r) = e\rho_\mu^p(r) \quad (2.30)$$

with source terms involving the various nucleonic densities and currents:

$$\rho_s(r) = \sum_{i=1}^{N} \bar{\psi}_i(r)\psi_i(r) \quad (2.31)$$

$$\rho_3(r) = \sum_{i=1}^{A} \psi_i^+(r)\tau_3\,\psi_i(r) \tag{2.32}$$

$$\rho_v(r) = \sum_{i=1}^{A} \psi_i^+(r)\psi_i(r) \tag{2.33}$$

$$\rho_p(r) = \sum_{i=1}^{A} \psi_i^+(r)\left(\frac{1-\tau_3}{2}\right)\psi_i(r) \tag{2.34}$$

$$j_\mu(r) = \sum_{i=1}^{A} \bar{\psi}_i(r)\gamma_\mu\psi_i(r) \tag{2.35}$$

$$\vec{j}_\mu(r) = \sum_{i=1}^{A} \bar{\psi}_i(r)\gamma_\mu\,\vec{\tau}\psi_i(r) \tag{2.36}$$

In the ground-state solution for an even-even nucleus spatial vector A(r) is neglected in the calculations, because the coupling constant of the electromagnetic interaction is small compared with the coupling constant of the mesons, and there are no currents (time-reversal invariance)[31].

The components of the vector ω and ρ mesons lead to the interactions between possible currents. For the ω meson the interaction is attractive for all combinations (pp, nn, pn), and for ρ mesons it is attractive for pp and nn currents but repulsive for pn currents [32].

The solution of the CDFT equations corresponds to the ground state of the nucleus it is corresponding to a local minimum in the potential energy surface, so to obtain the solution for any point we used the constrained of quadrupole mass moment. The constrained calculations were performed by imposing constraints on both axial and triaxial mass quadrupole moments [30]. The method of quadratic constraints uses an unrestricted variation of the function

$$\langle \widehat{H} \rangle + \sum_{\mu=0,2} C_{2\mu} \left(\langle \hat{Q}_{2\mu} \rangle - q_{2\mu} \right)^2 \tag{2.37}$$

Where $\langle \widehat{H} \rangle$ is the total energy and $\langle \widehat{Q_{2\mu}} \rangle$ is the expectation values of mass quadrupole operators,

$$\hat{Q}_{20} = 2z^2 - x^2 - y^2 \tag{2.38}$$

$$\hat{Q}_{22} = x^2 - y^2 \tag{2.39}$$

$q_{q\mu}$: is the constrained value of the multipole moment.

$C_{2\mu}$: is the corresponding stiffness constant [33].

2.4 The wavefunction

The CDFT equations are solved in the basis of an anisotropic three-dimensional harmonic oscillator in Cartesian coordinates characterized by the deformation parameters β_0 and γ and oscillator frequency $\hbar\omega_0 = 41A^{-1/3}$ MeV, for details see Refs. [36, 37].

They are solved in the parity, signature basis. Single-particle orbitals are labeled by $[Nn_z\Lambda]^{sign}$. $[Nn_z\Lambda]\Omega$ are the asymptotic quantum numbers (Nilsson quantum numbers) of the dominant component of the wave function at $\Omega_x = 0.0$ MeV. The superscripts sign to the orbital labels are used sometimes to indicate the sign of the signature r for that orbital ($r = \pm i$).

The self-consistent field σ, ω and ρ, are expanded into a complete set of eigenfunctions of the three-dimensional harmonic oscillator in Cartesian coordinates. The fields are written as:

$$\sigma(r) = \sum_N \sigma_N \phi_N(r) \tag{2.40}$$

$$\omega(r) = \sum_N \omega_N \phi_N(r) \tag{2.41}$$

$$\rho(r) = \sum_N \rho_N \phi_N(r) \qquad (2.42)$$

Where

$$\phi_N(r) = \phi_{n_x}(x)\phi_{n_y}(y)\phi_{n_z}(z) \qquad (2.43)$$

$$N = n_x + n_y + n_z \qquad (2.44)$$

$\hat{P}$ is the parity operator and $\hat{R}$ is the signature operator.

$$\hat{R}_x = e^{-i\pi \hat{j} x} \quad , \quad \widehat{R_x}\psi_i = r_i\psi_i \qquad (2.45)$$

with the eigenvalues are $r_i = \pm i$ The simplex operator is defined as:

$$\hat{S}_i = \hat{R}_i\hat{P} \qquad \text{i=x,y,z} \qquad (2.46)$$

$$P = S_x S_y S_z \qquad (2.47)$$

The positive simplex state is written as:

$$\Phi_K(r) = \phi_{n_x}(x)\phi_{n_y}(y)\phi_{n_z}(z)\frac{i^{n_y}}{\sqrt{2}}\begin{pmatrix}1\\(-)^{n_x+1}\end{pmatrix} \qquad (2.48)$$

The negative simplex state is written as:

$$\Phi_{\bar{K}}(r) = \phi_{n_x}(x)\phi_{n_y}(y)\phi_{n_z}(z)\frac{i^{n_y}}{\sqrt{2}}(-)^{n_x+n_y+1}\begin{pmatrix}1\\(-)^{n_x}\end{pmatrix} \qquad (2.49)$$

$$\Phi_{n_i}(x_i) = \left(\sqrt{\pi} 2^{n_i} n_i!\, b_i\right)^{-\frac{1}{2}} \exp\left(-\frac{1}{2}\left(\frac{x_i}{b_i}\right)^2\right) H_{n_i}\left(\frac{x_i}{b_i}\right) \qquad i = x, y, z$$

(2.50)

where H_{ni} are the Hermite polynomials.

2.5 Nuclear shape and deformation

The shape is one of the most fundamental properties of an atomic nucleus, along with its mass and radius.

The nuclear deformation can be measured by a multipole expansion for instantaneous coordinate R (t) of a point on the nuclear surface at (θ, φ) in terms of the spherical harmonics :

$$R(\theta, \varphi) = R_{avg}[1 + \sum_{\lambda} \sum_{\mu=-\lambda}^{\lambda} \alpha_{\lambda\mu} Y_{\lambda\mu}(\theta, \varphi)] \qquad (2.51)$$

When λ=0 that gives a monopole (spherical shape), and when λ=1 it gives dipole deformation, but the most important deviation from spherical shape is when λ=2, it is called quadrupole deformation. In this case we have five parameters$\alpha_{\lambda\mu}$, however, $\alpha_{21} = \alpha_{2-1} = 0$ and $\alpha_{22} =$

α_{2-2}, so the five parameters reduced to two real parameters α_{20} and α_{22} [2]

Where

$$\alpha_{20} = \beta \cos\gamma \tag{2.52}$$

$$\alpha_{22} = \frac{1}{\sqrt{2}}\beta \sin\gamma \tag{2.53}$$

We can connect the quadrupole constraint (2.38, 2.39) with β and γ

$$\beta = \sqrt{\frac{4\pi}{5}}\,\frac{Q}{r^2} \tag{2.54}$$

$$\gamma = tan^{-1}(\frac{Q_{22}}{Q_{20}}) \tag{2.55}$$

Where $$Q = \sqrt{Q_{20}^2 + Q_{22}^2} \tag{2.56}$$

If we substitute Eqs.(2.38,2.39) in Eq.(2.40), then we obtain

$$R(\theta,\varphi) = R_{avg}[1 + \beta\sqrt{\frac{5}{16\pi}}(\cos\gamma\,(3cos^2\theta - 1) + \sqrt{3}\,\sin\gamma\, sin^2\theta\cos 2\varphi)] \tag{2.57}$$

The increment on three axes can be calculated from eq. (2.46) as a function of β and γ :

$$R_x = R\left(\frac{\pi}{2}, 0\right) = R_{avg}[1 + \beta\sqrt{\frac{5}{4\pi}}\cos(\gamma - \frac{2\pi}{3})] \quad (2.58)$$

$$R_y = R\left(\frac{\pi}{2}, \frac{\pi}{2}\right) = R_{avg}[1 + \beta\sqrt{\frac{5}{4\pi}}\cos(\gamma + \frac{2\pi}{3})] \quad (2.59)$$

$$R_z = R(0,0) = R_{avg}[1 + \beta\sqrt{\frac{5}{4\pi}}\cos\gamma] \quad (2.60)$$

The quadrupole deformation can have axial symmetry, which two of three axes are equal. In that case, the nucleus have an ellipsoid shape with elongation along one axis and perpendicular cross section is circular. The shape is **prolate** when the nucleus elongated along z-axis and **oblate** when elongation is on x-axis or y-axis. The other case that the deformation can be without axial symmetry resulting in different elongations along the three axes of the system and the cross section is not circular, the shape is triaxial [34].

In general, when γ is multiple of 60° it has axial deformation as we can see from eqs. (2.47, 2.48, 2.49), which the two axes are equal:

If $\gamma = 0^{\circ}$ $R_x = R_y$

If $\gamma = 60^{\circ},\ R_x = R_z$

and if $\gamma = 120^{\circ}, R_y = R_z$

But when γ is not multiple of 60°, the nucleus have triaxial shape.

CHAPTER THREE
Structure of Cd isotopes

In this chapter we will perform unrestricted calculations for the search of the ground state minimum for Cd isotopic chain. We will consider both even and odd mass nuclei. Our calculations allows the nuclear shape to be spherical, axially deformed or triaxially deformed. For each nuclei, several physical observables will be calculated, and compared with the results obtained from other models and available experimental data. In addition to all of that both neutron drip line will be identified.

3.1 shape of Cd isotopic chain

We have carried out calculations for Cd isotopes with mass number A =95-164, which includes both even and odd mass nuclei. In our calculations the ground state shape can be spherical, axial (oblate or prolate) or triaxial. As mentioned in the previous chapter one, can categories the nuclei into two categories deformed and spherical. The

deformed nuclei can be either axial or triaxial depending on the value of gamma (eq.2.55). If $\gamma = 0^{\circ}$ the nucleus shape will be axial about the Z-axis and is called prolate. However, if γ is 60° or 120° the nucleus is still considered axial but this time the symmetry axis is the Y and the X axis, respectively, and the shape is called oblate. However, if γ is not a multiple of 60° there is no axial symmetry and the shape is traxial, that is there is no symmetry axis.

The nuclei will be categorized as prolate, oblate and triaxial, and the results are listed in Table 3.1.

TABLE 3.1: Cd isotopes (^{95}Cd to ^{164}Cd) listed in three columns according to their ground state shape; prolate, oblate and triaxial.

Prolate $(\gamma = 0^{\circ})$	**Oblate** $(\gamma = 60^{\circ} or 120^{\circ})$	**Triaxial** $(\gamma \; is \; not \; multipole \; of \; 60^{\circ})$
95	96	109
99	97	111
101	98	115

102	100	116
105	103	119
107	104	120
108	106	143
112	110	147
122	113	148
123	114	149
124	117	150
125	118	153
127	121	154
128	126	156
130	129	157
133	131	158
134	132	161
135	141	162
136	160	
137	163	
138		
139		
140		
142		
144		
145		
146		
151		
152		
155		
159		
164		

We notice from table 3.1 that the shape of nuclei from A=95 to 164 varies in several patterns. At the neutron deficient side of the chain, the ground state shape is axial. However, it alternate between prolate and oblate up to ^{108}Cd. Then from ^{109}Cd up to ^{122}Cd the shape keeps alternating between axial and triaxial forth and back. After that the shape is axial, but fluctuate between prolate and oblate shape, suddenly, at ^{143}Cd the shape become triaxial, next the shape still vary between tiaxial and axial (prolate shape) expect for 163Cd which have oblate shape.

The quadrupole deformation β_{20} is defined in the previous chapter (eq. 2.54). It provides an indication how the shape of nucleus is, and from calculations performed, we obtain values of β_{20} crossponding to ground state minimum for Cd isotopes. In figure 3.1: β_{20} is plotted as a function of mass number A. In this figure we notice that there are several jumps in different places which corresponds to A= [(97-98), (117-118), (129-130), (159-160) and 136] at these nuclei the value of β_{20} decrease sharply compared to those around it. The values of β_{20} related to these nuclei are ranging from 0.02 up to 0.05 except for A=136 for which β_{20}

is 0.09. This mean that at these nuclei, the nuclear shape becomes nearly spherical and the deformation disappear. However, for other nuclei the change is gradual and reaches a maximum value of 0.18. Our results are compared with those obtained from relativistic Hartree-Fock-Bogolibouve within Gogny -D1S[38] and we obtain a good agreement. Also we compared with results obtained using self-consistent mean field with choice of Skyrme force and pairing property and interacting boson model(IBM) for even – even $^{108\text{-}116}$Cd isotopes, the value of minimum $\beta_{20} = 0.15$ from these two model and small deviation exist when compared with our result[24].

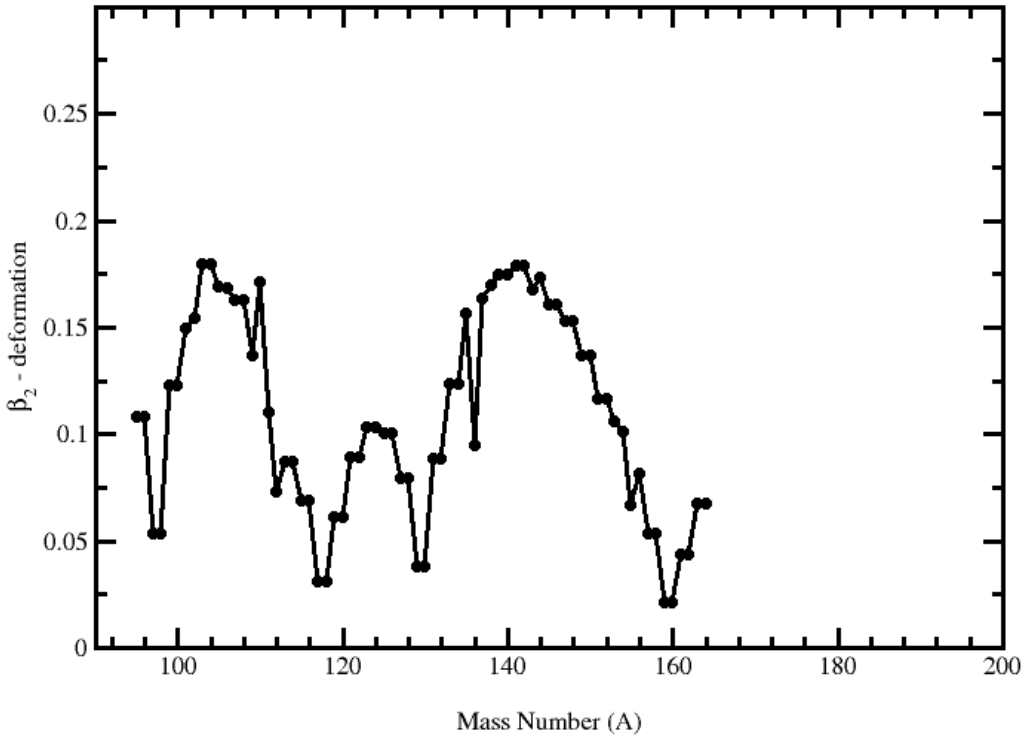

FIGURE 3.1: Quadrupole deformation parameters β20 for Cd isotopes as a function of mass number A=95 to164 using NL3* parametrization.

3.2 Single particle states

We pay attention to these nuclei where a jump in the value of deformations occurs. Due to that we plot single particle states for these

Cd isotopes where a jump in its β_{20} value occurs as seen in Figure 3.1 and two of its neighboring nuclei.

In Figure 3.2, we plot single particle states for $^{(96,\ 98,\ 100)}$Cd corresponding to values of β_{20}(0.10783, 0.05347, 0.12282), these isotopes have axial deformation as listed in table 3.1. These single particle states are compared with Nilsson diagram in ref. [39] and we obtained exactly the same states.

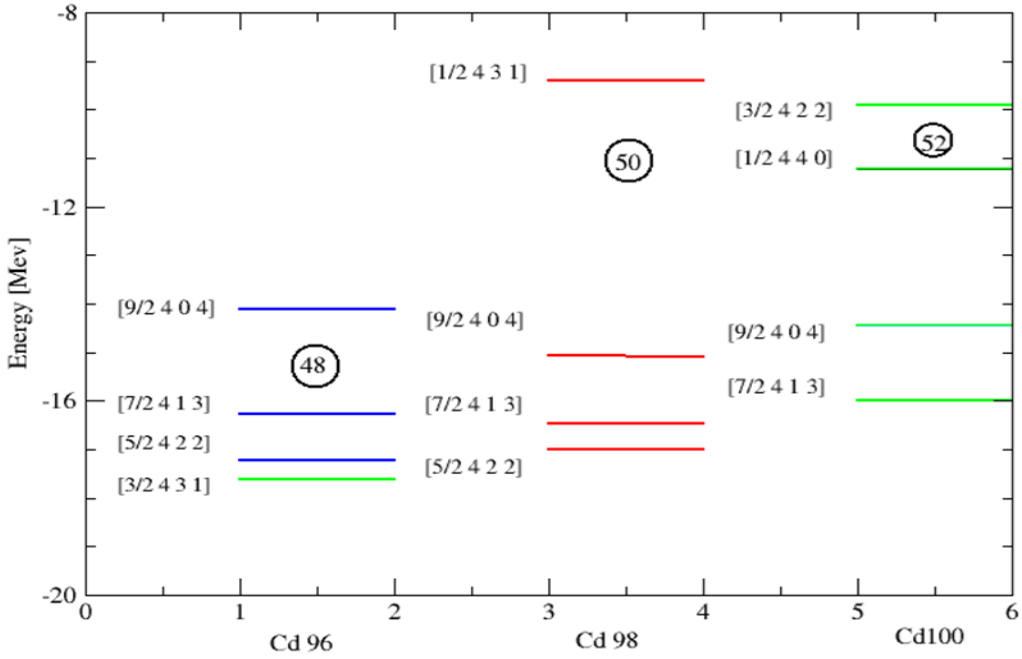

FIGURE 3.2: The Last three occupied states and first non-occupied one for Cd isotopes with A=96, 98, and 100.

However, in Figure 3.3, we draw single particle states for $^{(108, 109, 110)}$ Cd isotopes which ^{109,108}Cd are triaxial and ^{110}Cd is axial. When we compared to Nilsson diagram the ^{110}Cd has a good agreement but for $^{108, 109}$ Cd we find a difference between our result and Nilsson diagram [39]. This difference is due to triaxiallity in these nuclei, even for ^{108}Cd which its value of γ is close to 120°, the effect of small triaxillity on single particle states are clearer than its effect on the shape of nucleus.

The effect of triaxillity on single particle states can be explained as follows. The Nilsson labels are [N n_z Λ]Ω , where Ω is the projection of angular momentum on the symmetry axis, thus for axial deformation Ω is a good quantum number and the wave function ψ is a summation of N n_z Λ. However, for triaxiallity there is no symmetry axis and one can not project the angular momentum. Thus, Ω is no longer a good quantum number. The wave function ψ is a summation of Nn_z Λ Ω and this causing mixing between states with different Ω for more detail see ref. [40].

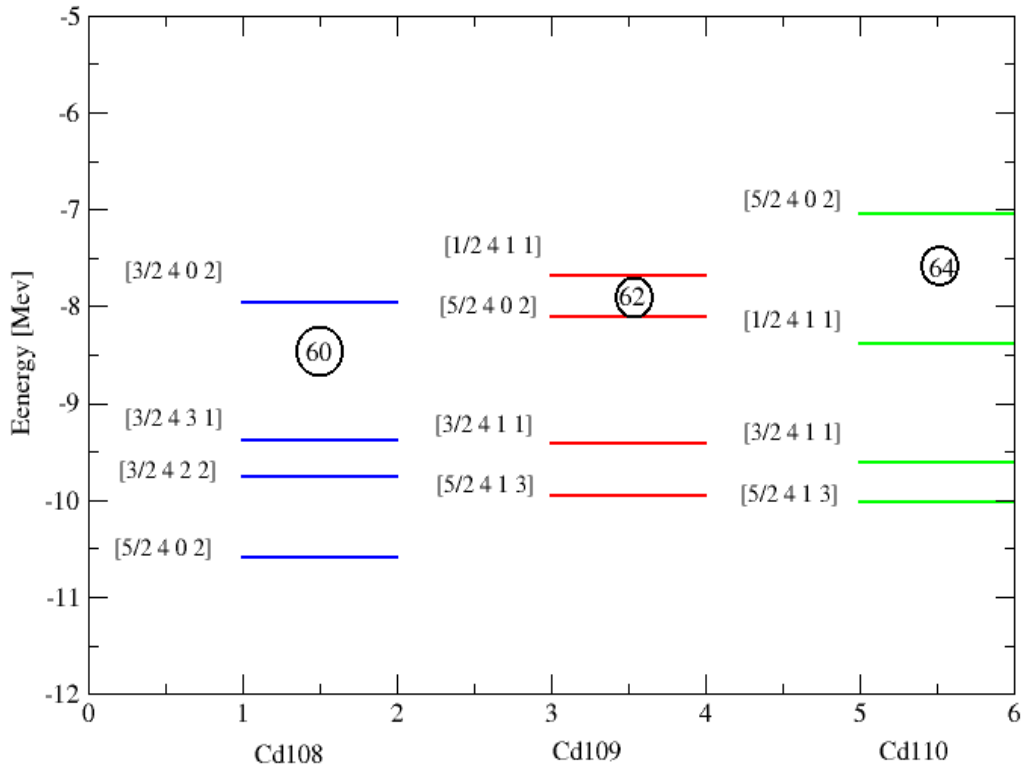

FIGURE 3.3: The Last three occupied states and first non-occupied one for Cd isotopes with A=108,109,110.

In figure 3.4, we plot single particle states for ^{116,118,120} Cd isotopes that have low values of β_{20} as we see from figure 3.1, which ^{118}Cd is the

minimum. According to table 3.1, the ^{118}Cd is axial but ^{116,120}Cd are triaxial. As we mentioned above, the triaxiallty has an effect on these states. So the states of these isotopes become incompatible with Nilsson

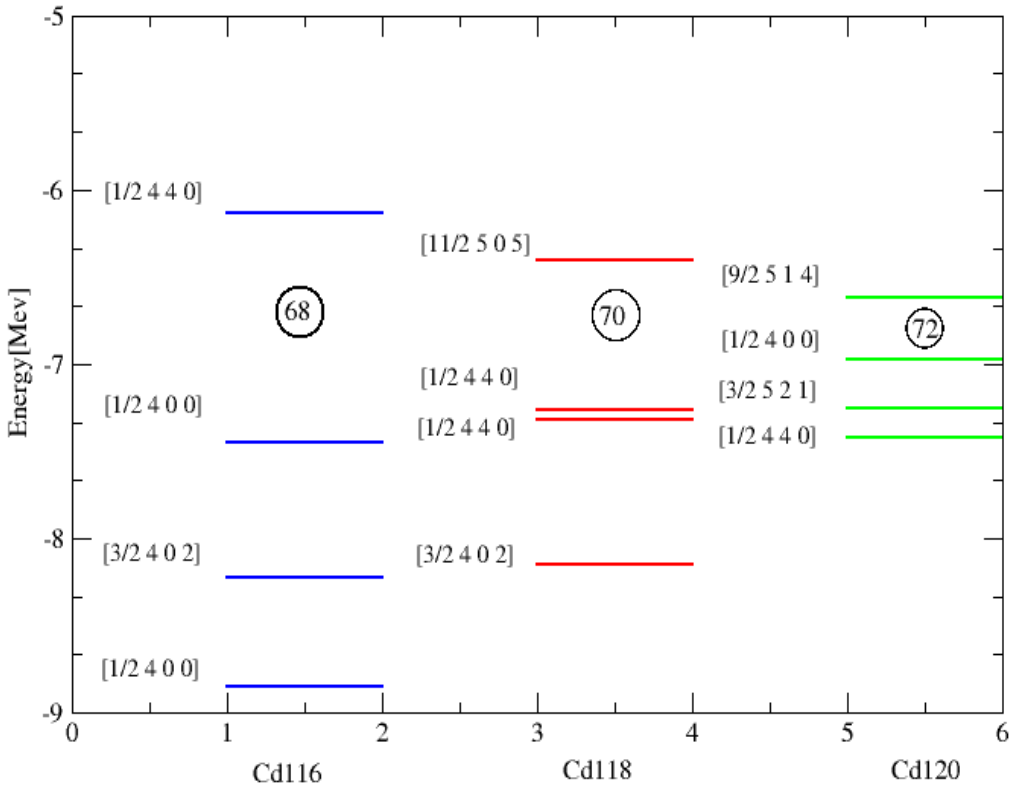

FIGURE 3.4: The Last three occupied states and first non-occupied one for Cd isotopes with A=116,118,120.

diagram, and they only become reliable in the limits of axial symmetry [40]. On the contrary the ^{118}Cd is in good agreement to Nilsson diagram because it is free from triaxiallty.

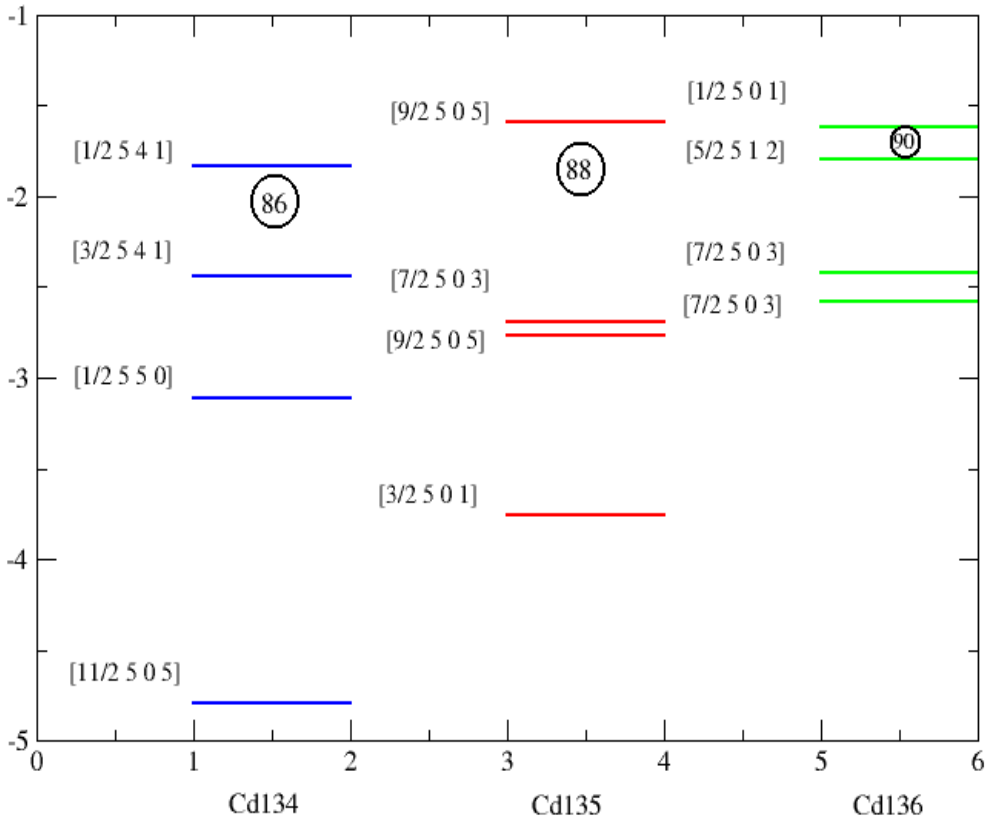

FIGURE 3.5: The Last three occupied states and first non-occupied one for Cd isotopes with A=134,135,136.

However, in figure 3.5, we plot states for ^{134,135,136}Cd isotopes that have high values of β_{20} compared to other isotopes in fig. 3.1, and here a max jump occur at ^{135}Cd. In addition, ^{134,135,136}Cd have axial symmetry and this is the reason for no difference occur between our results and Nilsson diagram [39].

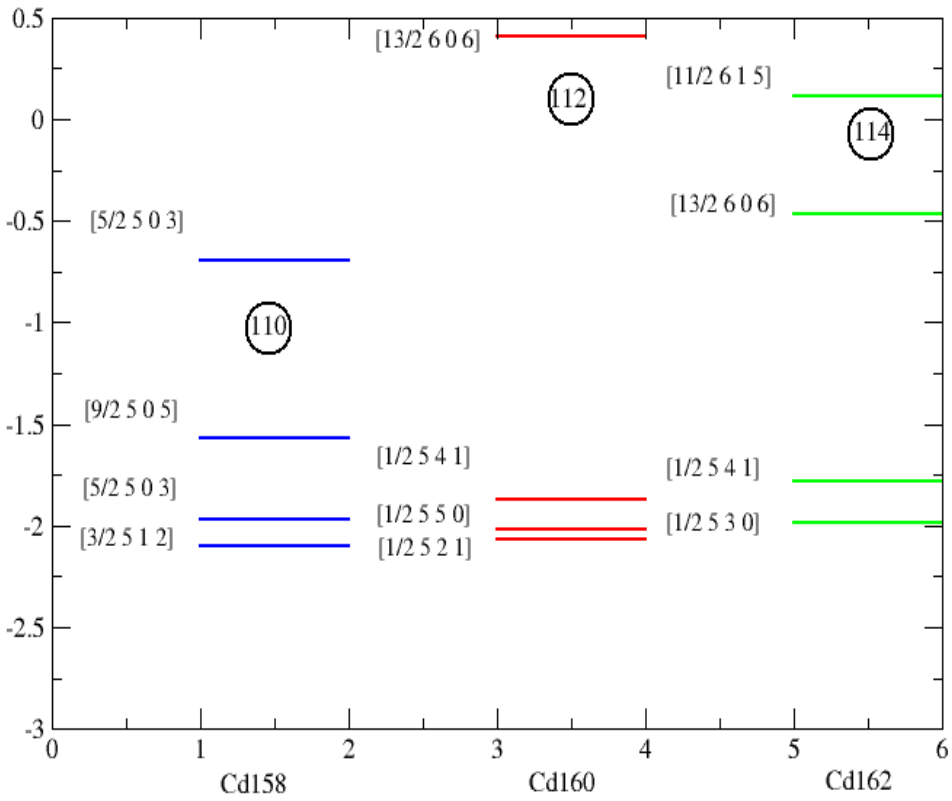

FIGURE 3.6: The Last three occupied states and first non-occupied one for Cd isotopes with A=158,160,162.

The last figure we plot for single particle states is figure 3.6, for ^{158,160,162} Cd isotopes which the smallest value of β_{20} occur at ^{160} Cd, also it has axial symmetry but ^{158,162} Cd isotopes around it having triaxial symmetry. So just ^{160}Cd is compatible to Nilsson diagram [39], but ^{158,162} Cd isotopes are not.

3.3 Physical properties of Cd isotopes

Physical properties are often referred to as observables that can be measured experimentally such as binding energy, two neutron separation energy, neutron and proton and charge radii.

3.3.1 Binding energy and two-separation energy

Binding energy is the energy required to disassemble the atomic nuclei into its main components (nucleons: proton and neutron). In Figure 3.8, the ground state binding energy per nucleon is plotted as a function of the mass number A. The results are shown for the NL3*

parametrization of the RMF Lagrangian. Our results in a very good agreement with the experimental data obtained from [34], and both shows to have the same trend. However, one can notice that there is small deviation for the odd-mass nuclei, and this deviation is small and does not exceed 0.2 MeV. From the figure, one also can conclude that the isotopes with mass number around 110 is the most stable one, which is because they have the highest binding energy per nucleon.

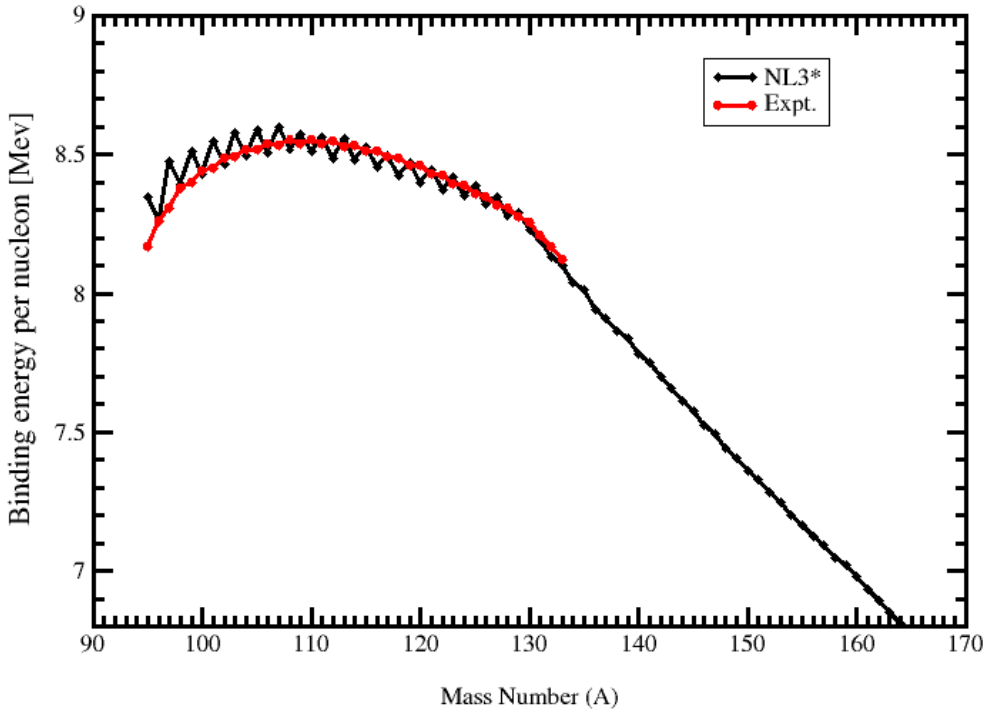

FIGURE 3.7: binding energy per nucleon for Cd isotopes using NL3* and experimental data [21] as a function of mass number A.

The two neutrons separation (S_{2n}) is the energy needed to remove two neutrons from a nucleus, and is given by:

$$S_{2n} = BE(^{A}_{Z}X_{N}) - BE(^{A}_{Z}X_{N-2}) \qquad (3.1)$$

The two-neutron separation energy is plotted as a function of mass number (A) in Figure 3.9. One can notice a smooth change in S_{2n} with A, except for A = 98,130 which corresponds to neutron number N = 50 and 82. These two number corresponds to magic numbers. At these two

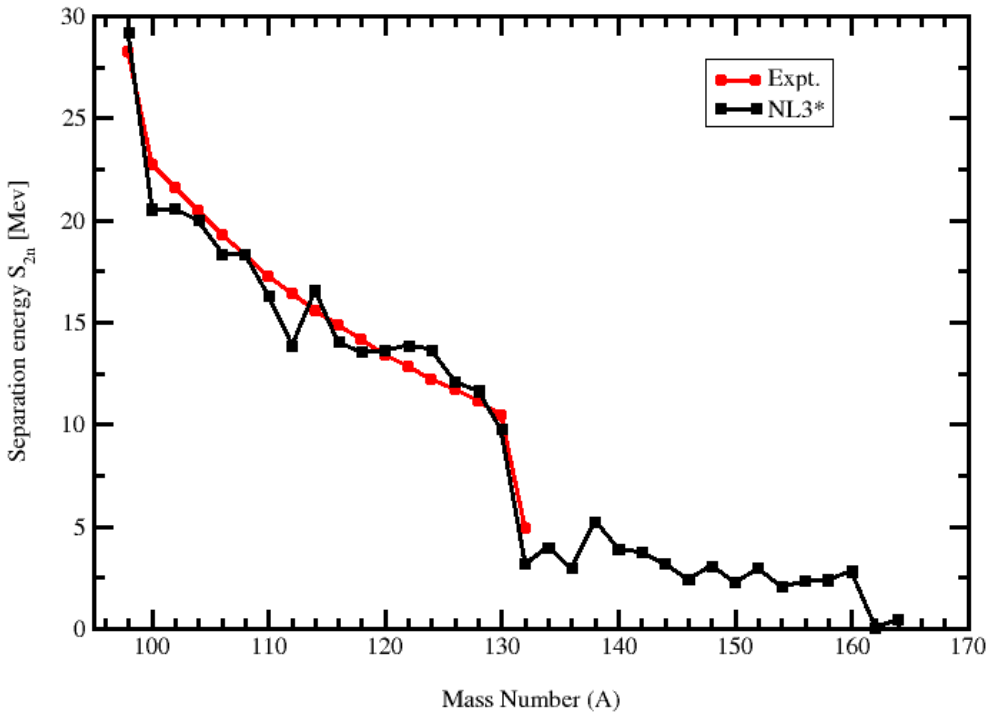

FIGURE 3.8: The two-neutron separation energy for even-even Cd isotopes using NL3* and experimental data [21] as a function of mass number A.

points a sharp and sudden change in S_{2n}occurs. This sharp jump can be attributed to two factor: The first one is due to the shell closure that occurs at N=50, 82, which as we know that the separation energy increases near shell closure. The second factor is the sudden change in the ground state shape from spherical shape ($\beta_2 \approx 0$) at ^{98,130}Cd to oblate shape at ^{100,132}Cd. This change in deformation strongly affect the last occupied state as compared with the spherical shape and might change the single particle occupation. Shape change significantly effects the two-neutron separation energy [14]. There is good agreement between our calculations and results obtained in experiment [34].

3.3.2 Neutron, proton and charge radius

In figure 3.10, we plot neutron and proton radius for Cd isotopes as a function of mass number A. We notice from the figure of neutron radius that the radius fluctuate up for odd isotopes and down for even isotopes. The reason for such a change is due to two factors. The first one is when we add a neutron to an even core of neutrons this means that a new

orbital must be opened and filled with this neutron, and thus an increase in the nuclear size. However, when we add a neutron to an odd core of neutrons, it will occupy the same orbital as in the previous neutron. In addition to that, the extra neutron reduces the coulomb repulsion between the protons and this causes the nucleons to come closer to each other. Thus reducing the neutron radius.

However, the bottom panel of fig.3.10 shows that proton radius has a different pattern from neutron radius. Although the number of proton is constant, we observe an increase in radius in general; this is due to increase the number of neutron for Cd isotopes, so the distribution of proton changes. In addition, we notice that the most of neighboring nuclei have the same radius. When comparing with the corresponding value of deformation shown in figure 3.1, we notice that these nuclei have same value of β_{20}. On the contrary, for ^{136}Cd the radius decreases. This

is because of value of β_{20} for it, which decline sharply, compared with nuclei around it.

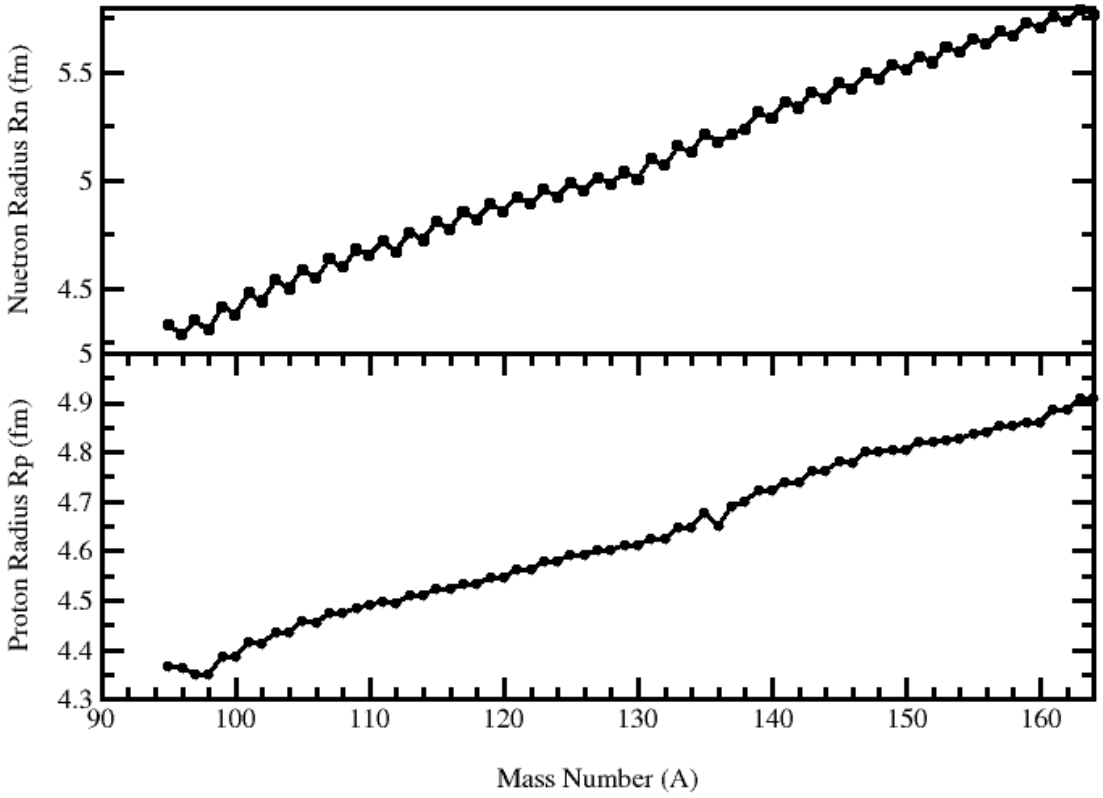

FIGURE 3.9: Radius of neutron and proton for Cd isotopes as a function of mass number using NL3*.

One of the most fundamental properties of the atomic nuclei is the nuclear charge radius. It plays a key role in studying the characters of nucleus and testing theoretical models. It is calculated by this formula

$$R_C = \sqrt{R_p^2 + 0.64} \qquad 3.2$$

Where 0.64 is related to finite volume of the proton (volume correction).

The charge radius follows the same behavior as the proton radius.

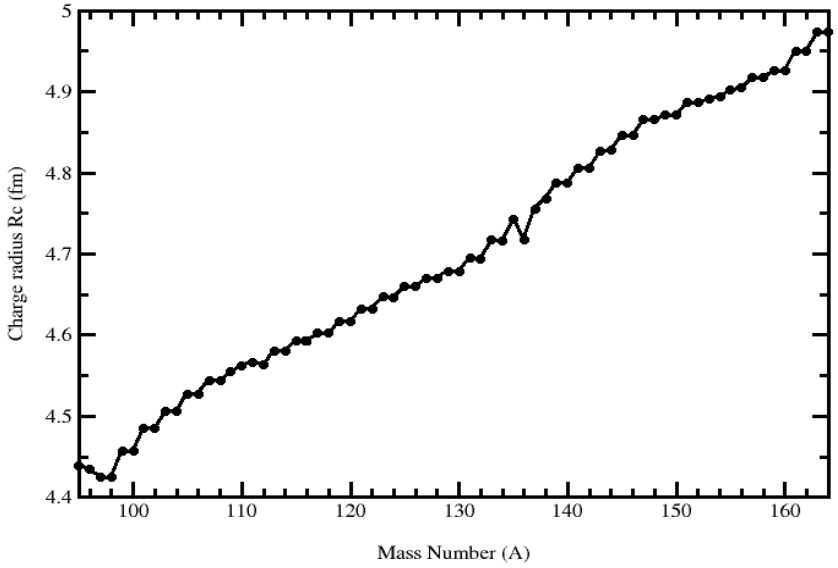

FIGURE 3.10: Charge radius for Cd isotopes as a function of mass number (A) using NL3*.

CHAPTER FOUR
Conclusion

In this thesis relativistic mean field theory (RMFT) using nonlinear meson nucleon coupling model has been successfully applied to investigate the shape of ground state for Cd (Z=48, $47 \leq N \leq 116$) isotopes and the physical properties such as binding, two neutron separation energies and proton and neutron radii.

We perform unrestricted calculations for the search of the ground state minimum for Cd isotopes. Our calculation allows the nuclear shape to be spherical, axially or triaxillity deformed.

The nuclear shape of Cd isotopes varies between two categories axial and triaxial shape. This is depend on value of γ. If γ=0° the shape is axial (prolate), if $\gamma = 60^{\circ} or\ 120^{\circ}$ the shape is also axial but (oblate) and if γ is not a multiple of $60^{\circ}$the shape is triaxial.

We also depended on value of quadrupole deformation β_{20} to study the shape of Cd isotopes. We plotted it as afunction of mass number A. From figure, we notice that value of β_{20} for some nuclei goes to zero, this mean that their shape become nearly spherical. In addition, we depend on value of β_{20} to choose nuclei, which we plot single particle states for them. We compared our states with Nilsson diagram and got a good agreement for axial nuclei but for triaxial nuclei the states are different.

One can see that the shape of nuclei has an effect on physical properties in the ground state. We notice a smooth change in physical properties in general. The sharp jump in most physical properties is observed at A=98, 130, 136. This sharp jump is due to change the shape of the ground state in the neighboring nuclei for these Cd isotopes.

References

[1] S. Frauendorf, AIP Conference Proceedings 1753, 030001 (2016)

[2] A. Bohr and B. Mottelson Nuclear Structure Vol. II. Nuclear Deformations, (W. A. Benjamin Inc., London/Amsterdam; Don Mils, Ontario/Sydney/Tokyo;(1975).

[3] Y.X. LUO et al. Rom. Journ. Phys., Vol. 57, Nos. 1–2, P. 309–329, Bucharest, 2012

[4] John L. Wood, EPJ Web of Conferences, 93 01006 (2015)

[6] Andreas Gorgen, and Wolfram Korten, Journal of Physics G Nucl. and Part. Phys., 43(2), 024002 (2016).

[7] A. Arima and F. Lachello, Adv. in Nucl. Phys., Vol. (13), (139-140), 1984.

[8] O. Scholten, Phys. Rev. C 28, 1783 (1983).

[9] R. L. Hatch and S. Levit, Phys. Rev. C 25, 614 (1982).

[10] Michael Bender, et al, Phys. Rev. Mod. 75, 121 (2003).

[11] J. W. Negele, Phys. Rev. Mod. 54, 913 (1982).

[12] Balazs Rozsnyai, Phys. Rev. 124, 860 (1961).

[13] Wen Hui Long, et al, Phys. Rev. C 81, 024308 (2010).

[14] N. Abuawwad, shape coexistence in Germanium and Selenium isotopes using covariant density functional theory, Palestine, (2018)

[15] Wen Hui Long, et al, Phys. Rev. C 81, 024308 (2010).

[16] T. Niksic, N. Paar, Comp. Phys. Com., 185, 18081821 (2014).

[17] Imam Hossain, Hewa Y Abdullah, Imad M Ahmed and Mohammad A Saeed, Jour. of Theo. and App. Phys., 1-5, (2013).

[18] P.E. Garrett, EPJ Web of Conferences, 66, 02039 (2014).

[19] Michael Hammen, Spins, Moments and Radii of Cd Isotopes, Mainz, 2013.

[20] O. V. Bespalova, B. S. Ishkhanov, A. A. Klimochkina, A. A. Kostyukov, E. A. Romanovsky, and T. I. Spasskaya, Bulletin of the Russian Academy of Sciences. Physics, Vol. 78, No. 5, pp. 401–404 (2014)

[21] A. Blazhev,a, K. Heyde, J. Jolie, and T. Schmidt, EPJ Web of Conferences, 93, 0101 (2015).

[22]K. C. Naik1, R. N. Panda1, and S. K. Patra, Nucl. Phys. 63 (2018)

[23] G. Saxena, M. Kaushik, 1608. 04505, (2016)

[24] K. Nomura, J. Jolie, Phys Rev. C. 98. 024303, (2018)

[25] P Ring, J. Phys.: Conf. Ser. 205 012010, (2010)

[26] P. W. Zhao, L. L. Li, Z. P. Li, Z. M. Niu, P. Ring, J. M. Yao, S. G. Zhou, and J. Meng, EPJ Web of Conferences, 38 02001 (2012)

[27] W. Pannert, P. Ring, and J. Boguta, Phys. Rev. Lett. 59, 2420 (1987)

[28] J. Boguta and A. R. Bodmer, Nucl. Phys. A292, 413 (1977).

[29] G. A. Lalazissis, S. Karatzikos, R. Fossion, D. Pena Arteaga, A. V. Afanasjev, P. Ring, Phys. Lett. B671, 36 (2009).

[30] H. Abusara, Shakeb Ahmad, and S. Othman, Phys. Rev. C 95, 054302 (2017)

[31] Y. K. Gambhir, P. Ring, and A. Thimet, ANYALS OF PHYSICS 198, 132-179 (1990).

[32] Y. K. Gambhir, and P. Ring, Mod. Phys. Lett. A 9, 787-795 (1993).

[33] Abu sara, Hazem, NUCLEAR PHENOMENA IN COVARIANT DENSITY FUNCTIONAL THEORY, Mississippi State University, Mississippi State, Mississippi, 2011

[34] M. Wang et al., Chin. Phys. C 36, 1603 (2012).

[35] K. C. Naik1, R. N. Panda1, and S. K. Patra, Proceedings of the DAE Symp. on Nucl. Phys. 63 (2018)

[36] A. V. Afanasjev, J. K¨onig and P. Ring, Nucl. Phys. A608, 107 (1996).

[37] W. Koepf and P. Ring, Nucl. Phys. A493, 61 (1989).

[38] http://www-phynu.cea.fr/HFB-Gogny_eng.htm.

[39] http://www.lnl.infn.it/~pisolo/alberto/Nilsson_Diagrams.pdf

[40] S. Nillson and I. Ragnarsson, Shape and shells in nuclear structure, Combridge university Press, New York, (1995).